Neuro-Oncology
20(9), 1197–1206, 2018 | doi:10.1093/neuonc/noy051 | Advance Access date 5 April 2018

Modeling the diffusion of D-2-hydroxyglutarate from IDH1 mutant gliomas in the central nervous system

Andreas Linninger, Grant A. Hartung, Benjamin P. Liu, Snezana Mirkov, Kevin Tangen, Rimas V. Lukas, Dusten Unruh, C. David James, Jann N. Sarkaria, and Craig Horbinski

Department of Bioengineering, University of Illinois at Chicago, Chicago, Illinois (A.L.); Department of Neurosurgery, University of Illinois at Chicago, Chicago, Illinois (A.L., G.A.H., K.T.); Department of Radiology, Northwestern University, Chicago, Illinois (B.P.L.); Department of Neurological Surgery, Northwestern University, Chicago, Illinois (S.M., D.U., C.D.J., C.H.); Department of Neurology, Northwestern University, Chicago, Illinois (R.V.L.); Mayo Clinic, Rochester, Minnesota (J.N.S.); Department of Pathology, Northwestern University, Chicago, Illinois (C.H.)

Corresponding Author: Craig Horbinski, M.D., Ph.D., Tarry 2-705, 300 East Superior Street, Chicago, IL 60611 (craig.horbinski@northwestern.edu).

Abstract

Background. Among diffusely infiltrative gliomas in adults, 20%–30% contain a point mutation in isocitrate dehydrogenase 1 (IDH1^{mut}), which increases production of D-2-hydroxyglutarate (D2HG). This is so efficient that D2HG often reaches 30 mM within IDH1^{mut} gliomas. Yet, while up to 100 μM D2HG can be detected in the circulating cerebrospinal fluid of IDH1^{mut} glioma patients, the exposure of nonneoplastic cells within and surrounding an IDH1^{mut} glioma to D2HG is unknown and difficult to measure directly.

Methods. Conditioned medium from patient-derived wild type IDH1 (IDH1^{wt}) and IDH1^{mut} glioma cells was analyzed for D2HG by liquid chromatography–mass spectrometry (LC-MS). Mathematical models of D2HG release and diffusion around an IDH1^{mut} glioma were independently generated based on fluid dynamics within the brain and on previously reported intratumoral and cerebrospinal D2HG concentrations.

Results. LC-MS analysis indicates that patient-derived IDH1^{mut} glioma cells release 3.7–97.0 pg D2HG per cell per week. Extrapolating this to an average-sized tumor (30 mL glioma volume and 1×10^8 cells/mL tumor), the rate of D2HG release by an IDH1^{mut} glioma (S_A) is estimated at $3.2–83.0 \times 10^{-12}$ mol/mL/sec. Mathematical models estimate an S_A of $2.9–12.9 \times 10^{-12}$ mol/mL/sec, within the range of the in vitro LC-MS data. In even the most conservative of these models, the extracellular concentration of D2HG exceeds 3 mM within a 2 cm radius from the center of an IDH1^{mut} glioma.

Conclusions. The microenvironment of an IDH1^{mut} glioma is likely being exposed to high concentrations of D2HG, in the low millimolar range. This has implications for understanding how D2HG affects nonneoplastic cells in an IDH1^{mut} glioma.

Key words

D-2-hydroxyglutarate | glioma | IDH1 | microenvironment | mathematical modeling

A subset of gliomas contain point mutations in isocitrate dehydrogenase 1 (IDH1) or IDH2 (collectively referred to as IDH1^{mut}). Wild-type IDH1 (IDH1^{wt}) oxidizes isocitrate into α-ketoglutarate (αKG), but IDH1^{mut} heterodimerizes with IDH1^{wt} and converts αKG into D-2-hydroxyglutarate (D2HG).[1] This process is so efficient that the concentration of D2HG in IDH1^{mut} glioma homogenates is usually between 10 and 30 mM.[2] D2HG appears to be a major intracellular effector of the IDH1^{mut} phenotype, inducing global histone and DNA hypermethylation, increasing oxidative stress, and impairing DNA repair.[1,3]

In addition to its effects within tumor cells, D2HG may also affect nonneoplastic cells in and around IDH1^{mut} tumors. In experimental models, D2HG traffics out of

Importance of the study

While it is increasingly becoming clear that the D2HG product of IDH1^{mut} enzyme is released by glioma cells into the tumor microenvironment and has considerable activities outside the tumor cell, it is difficult to obtain precise in vivo measurements of D2HG concentration in the extracellular compartment without artefactual disruption of the cells and tissues. Herein, we describe estimates of the extracellular D2HG concentration gradient using 2 complementary approaches, one based on D2HG release from cultured IDH1^{mut} glioma cells, and the other based on mathematical models using known concentrations of D2HG within tumor lysates and the cerebrospinal fluid of patients. Both approaches generated similar results, suggesting that the extracellular concentration of D2HG is likely in the low millimolar range in the immediate tumor microenvironment. This will have profound implications for the growing field of research that explores the effects of D2HG on nonneoplastic cells in and around IDH1^{mut} gliomas.

IDH1^{mut} cells in vitro and in vivo,[2,4] albeit through unknown mechanisms, and is readily detected in the cerebrospinal fluid (CSF) of IDH1^{mut} glioma patients at levels up to 100 μM.[5] Exogenous D2HG causes oxidative stress, inhibits expression of pro-apoptotic proteins, reduces pro-inflammatory signaling, and alters cellular metabolism.[6–11] Our recent studies found that D2HG can also inhibit platelet aggregation and increase neuronal network firing, correlating with reduced intratumoral microthrombi and increased seizure risk, respectively.[12,13] However, the full impact of D2HG as a modulator of the tumor microenvironment remains unclear, because it is difficult to accurately quantify the concentration of interstitial D2HG within an intact IDH1^{mut} tumor without physically damaging the tissue and disrupting tumor cells.

In the current study, we employed 2 independent approaches, quantifying the release rate of D2HG in patient-derived IDH1^{mut} glioma cells and mathematical modeling of intracerebral D2HG diffusion, in order to develop an evidence-based estimate of the D2HG concentration gradient in the extracellular fluid surrounding IDH1^{mut} gliomas. Both approaches produced similar results, thereby providing a rationale on which to base experiments addressing the impact of D2HG in the tumor microenvironment.

Materials and Methods

Patient-Derived Glioma Cells

Patient-derived glioma cells with endogenous IDH1^{mut} were obtained from Dr Jann Sarkaria at Mayo Clinic (GBM164 and GBM196), Dr Hai Yan at Duke University (TB09), and American Type Culture Collection (ATCC) (BT142). IDH1^{mut} HT1080 fibrosarcoma cells were also acquired from ATCC. GBM164, TB09, and BT142 express R132H IDH1, as confirmed by western blot (not shown). HT1080 cells express R132C IDH1. IDH1^{wt} gliomas included GBM6, GBM12, and GBM43. The unique identity of each of these cell types has been validated via short tandem repeat PCR. Cells were plated in triplicate at 250 000/well in 6-well plates, with 2 mL of culture medium per well. GBM6, GBM12, GBM43, and HT1080 cells were grown in Eagle's minimal essential medium (Corning #10-009-CV) with 10% fetal bovine serum (FBS) and 1% penicillin/streptomycin. GBM164, GBM196, TB09, and BT142 cells were cultured in 1:1 Dulbecco's modified Eagle's medium (Gibco #11965092) and NeuroCult NS-A Basal Medium (Stem Cell Technologies #05750), supplemented with NeuroCult NS-A proliferation supplement (Stem Cell Technologies #05753), 10% FBS, 1% penicillin/streptomycin, heparan sulfate (1 μg/mL), fibroblast growth factor (5 ng/mL), and epidermal growth factor (10 ng/mL).

After 7 days, the conditioned medium was collected for D2HG quantification, cells were washed with phosphate buffered saline (PBS), detached with trypsin, and centrifuged at 500 *g* for 5 min. Cell pellets were resuspended in PBS, and cells were counted in a trypan blue exclusion assay with a hemocytometer.

D2HG Quantification via Liquid Chromatography–Mass Spectrometry

Culture media samples were analyzed using an AB Sciex Qtrap 5500 MS coupled to an Agilent 1260 Ultra Performance Liquid Chromatography (UPLC) system, with a Waters ACQUITY UPLC Ethylene Bridged Hybrid (BEH) C18 Column, 130 Å, 1.7 μm, 2.1 mm × 100 mm, at a flow rate of 500 μL/min. A linear gradient of 1%–60% buffer B (100% MeOH) was applied. Mass spectrometry (MS) data were acquired by multiple reaction monitoring scan (negative electrospray ionization voltage 4.5 kV, temperature 400°C, m/z range 50–300) monitoring signature product ions 147>85 (Quantifier) and 147>101 (Qualifier) transitions. Quantification was achieved using peak area of monitored transitions.

D2HG from Sigma-Aldrich (catalog #H8378) was used to develop a liquid chromatography (LC)–MS standard curve. D2HG was serially diluted in MS-grade 1:1 methanol:water solution. Then, a standard curve was created with 7 points: 50 pg/mL, 200 pg/mL, 500 pg/mL, 2 ng/mL, 5 ng/mL, 50 ng/mL, and 200 ng/mL D2HG. Each point was spiked with 25 ng/mL stable isotope-labeled $^{5}C_{13}$ D2HG standard (catalog #793272, Sigma). All D2HG standard curve samples and conditioned medium samples were analyzed in triplicate, with a blank run followed by each sample run using the same gradient. Using this approach, the D2HG standard curve showed extremely high linearity, with R = 0.999.

Mathematical Modeling of Intracerebral D2HG Diffusion

A numerical model of the reaction-diffusion in Equation (1) (below) was created using an idealized radially symmetric model. The radius (r) of the spherical system covers the concentric compartments as in Fig. 2. This steady-state species balance equates the diffusive flux with the production rate of D2HG. Here the concentration in each volume of D2HG is C_A, and the diffusion coefficient is D_i. The D2HG production rate of the compartment is given by a zeroth order reaction rate, $V_i S_{A,i}$, where V_i is the volume of the element. The production rate ($S_{A,i}$) is equal to $\overline{S_A}$ in the tumor domain (Ω_t). In the other 2 compartments, brain tissue (Ω_b) and CSF (Ω_{csf}), there is no D2HG production and hence the reaction rate is 0.

IDH1^{mut} gliomas produce D2HG, which spreads by diffusion radially through the brain tissue into the CSF compartment. D2HG is cleared from the CSF by passive transport together with the reabsorbed CSF (unhindered clearance) with the flux of D2HG into the CSF (f_{CSF}) defined as a function of CSF bulk flow (q_{CSF}) and the concentration of the solute in the CSF ($C_{A,\,CSF}$) given in Eq. (2). Symmetry is assumed at the center of the tumor mass.

$$\vec{\nabla} D_i \vec{\nabla} C_{A,i} + V_i S_{A,i} = 0 \tag{1}$$

$$\begin{cases} S_{A,i} = \overline{S_A} & x \epsilon\, \Omega_t \\ S_{A,i} = 0 & x \epsilon\, \Omega_b, \Omega_{CSF} \end{cases}$$

$$f_{CSF} = q_{CSF}\, C_{A,CSF} \tag{2}$$

The rate of D2HG release by the tumor was predicted using mass conservation between production and clearance, as reflected by Eq. (3). The parameters used can be seen in Table 1 alongside the predicted range of D2HG release rate in the tumor mass.

$$S_A V_t - f_{CSF} = 0 \tag{3}$$

The steady-state calculation was formulated in spherical coordinates and solved using MatLab (MathWorks). The spherical model was implemented with both a finite element method and a finite volume method. These methods were in agreement and were each validated with a mesh independence study. Mesh independent profiles were achieved with about 201 volume elements (see Supplementary material). The calculations in MatLab for a single curve is 24.2 seconds on a standard desktop computer for 2001 total volume elements.

We extended the transport equations to 2 three-dimensional models using subject-specific geometries. The brain matter and corresponding tumor mass were reconstructed from medical images from MRI scan using FreeSurfer (https://surfer.nmr.mgh.harvard.edu/). Patient 1 was a 24-year-old man who presented with seizures and on MRI was found to have a right frontal lobe tumor mass that was surgically resected and diagnosed as a grade III astrocytoma harboring the IDH1 mutation. Patient 2 was a 37-year-old woman who also presented with a seizure, as well as a right frontal lobe IDH1^{mut} grade III astrocytoma. Presurgical/pretreatment MRI of the subject brain and tumor were used for mathematical modeling to avoid confounding factors due to surgery and treatment. Utilized for modeling were fluid attenuated inversion recovery and high resolution 1 mm slice thickness gadolinium contrast-enhanced magnetization-prepared rapid acquisition with 3D gradient echo pulse sequences. The 3D reconstructed model included 882 270 and 7 363 422 volume elements for the tumor and brain material, respectively, for patient 1 and 932 124 and 6 089 840 volume elements for the tumor and brain material, respectively, for patient 2. D2HG production and its perfusion through the tissue were simulated with ANSYS software using the same parameters as those chosen in the spherical model.

Results

Quantification of D2HG Release from IDH1^{mut} Glioma Cells

To more accurately estimate how much D2HG is released by IDH1^{mut} glioma cells into their microenvironment, we used LC-MS to quantify the amount of D2HG released by in vitro patient-derived IDH1^{mut} glioma cells into culture medium.

Table 1. Model parameters used to predict D2HG release rate (S_A)

Parameter	Symbol	Value	Units
Tumor radius	r_{tumor}	1.5299	cm
CSF concentration	c_{CSF}	0.0075–0.1 × 10^{-6}	mol/cm^3
CSF flow rate	q_{CSF}	500	cm^3/day
Predicted production rate	S_A	2.894–12.867 × 10^{-12}	mol/cm^3/s
Diffusion coefficients in tumor	D_t	0.5 × 10^{-6}	cm^2/s
Diffusion coefficients in brain tissue	D_b	0.5 × 10^{-6}	cm^2/s
Diffusion coefficients in CSF space	D_{CSF}	0.75–30.2 × 10^{-6}	cm^2/s

After one week, GBM164 cells released an average of 4.5 µg D2HG into 2 mL of culture medium. Based on cell counts, this equated to approximately 3.7 pg D2HG released by each GBM164 cell/week, whereas TB09 cells released 6.7 pg D2HG/cell/week (Fig. 1). GBM196 released much more D2HG than either GBM164 or TB09, at 97.0 pg/cell/week. As expected, the average amount of D2HG released by IDH1^{wt} glioma cells was much lower, at 0.29 pg/cell/week. Only 0.77 pg D2HG was released per IDH1^{mut} BT142 glioma cell, because this cell line no longer expresses IDH1^{wt}, and a wild-type:mutant heterodimer is required for elevated D2HG production.[14] These data therefore suggest that when the 1:1 IDH1^{wt}:IDH1^{mut} heterodimer stoichiometry is lost, as often occurs during IDH1^{mut} glioma progression,[15] D2HG release is markedly reduced. In contrast, IDH1^{mut} HT1080 sarcoma released 15.1 pg D2HG/cell/week.

Translating these in vitro findings to patient tumors, a prior report estimated that the average cell density in solid tumors is at least 1×10^8 cells per mL wet tissue volume.[16] Based on our patient-derived IDH1^{mut} glioma cells (excluding HT1080 fibrosarcoma cells) and an estimated average tumor volume of 30 mL (4 cm diameter, assumed spherical shape), the total rate of D2HG release (S_A) of a typical IDH1^{mut} glioma was therefore estimated to be 3.2–83.0×10^{-12} moles of D2HG per second.

Mathematical Modeling of D2HG Release and Spread Around an IDH1^{mut} Glioma

Separate from the quantification of D2HG release in cultured IDH1^{mut} glioma cells described above, we developed estimates of D2HG diffusion from an IDH1^{mut} glioma, based on known properties of CSF turnover, intracerebral fluid flow, diffusion of small polar compounds like D2HG, the concentration of D2HG within homogenates of IDH1^{mut} gliomas, and the levels of D2HG within the CSF of IDH1^{mut} glioma patients.[2,5] Using Eqs. (1)–(3), the idealized radially symmetric model shown in Fig. 2, and the parameters listed in Table 1, we simulated a range of D2HG release rates (S_A) and D2HG diffusivity constants within the tumor, brain, and CSF (Fig. 3). These simulations generated a range of D2HG concentrations in a 2 cm radius around an IDH1^{mut} tumor, with a consistently rapid drop in D2HG away from the tumor center. At all the simulated diffusion constants, D2HG release rates in the range of 2.9–12.9×10^{-12} mol/sec generated curves that fit the previously reported steady-state concentrations of D2HG within IDH1^{mut} gliomas,[2] as well as the range of D2HG previously detected in the CSF of IDH1^{mut} glioma patients.[5] This range of D2HG release rates was within the rates that were independently extrapolated from in vitro data, 3.2–83.0×10^{-12} mol/sec (Fig. 2), strengthening the validity of these mathematical models.

Based on the steady-state formula in Eq. (3) and the parameters tested in Fig. 3 using a spherical coordinate system simulation, we produced two rigorous 3D computational fluid dynamic (CFD) models using detailed patient-specific reconstructions of brain tissue and tumor mass. This produced a D2HG concentration profile that followed the spherical model pattern, incorporating brain anatomy and a common IDH1^{mut} glioma size and location (Figures 4 and 5). For this model, the diffusivity in the tumor, brain, and CSF compartments, the D2HG production rate, and the CSF boundary flux value can be seen in Table 2. In this model, the reconstructed volume of the brain tissue is 1508 mL and the resulting spread of D2HG above a toxic threshold covered a volume of 110.8 mL. In this model, approximately 7.3% of the cerebrum is likely being exposed to low millimolar levels of D2HG, which we recently demonstrated were sufficient to increase synchronized network bursts in cultured cortical neurons.[17]

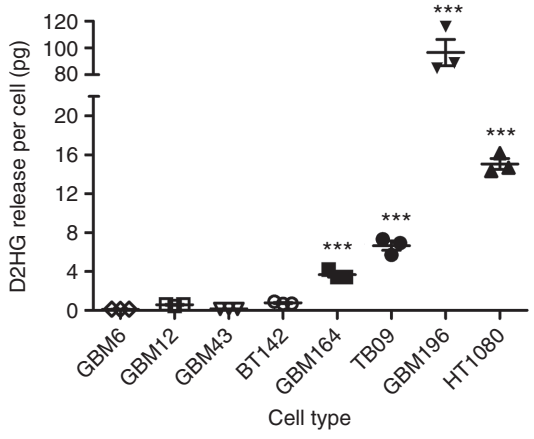

Fig. 1. In vitro D2HG release by IDH1^{wt} and IDH1^{mut} cells. Glioma cells consisted of IDH1^{wt} (GBM6, GBM12, GBM43), homozygous IDH1^{mut} (BT142), and heterozygous IDH1^{mut} (GBM164, TB09, GBM196). HT1080 are heterozygous IDH1^{mut} fibrosarcoma cells. See "Materials and Methods" for details on cell culture conditions and LC-MS analysis of D2HG. ***$P < 0.0001$ compared with GBM6, GBM12, GBM43, and BT142 cells by one-way ANOVA.

Discussion

The interaction between neoplastic cells and their microenvironment forms the underpinnings of several hallmarks

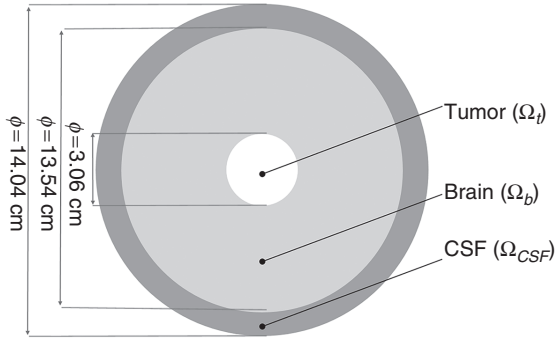

Fig. 2. Schematic representation of the idealized system. White delineates the tumor domain (Ω_t) with a diameter of 3.06 cm, light gray is the brain matter (Ω_b) with a diameter of 13.54 cm, and dark gray is the CSF compartment (Ω_{CSF}) with a diameter of 14.04 cm.

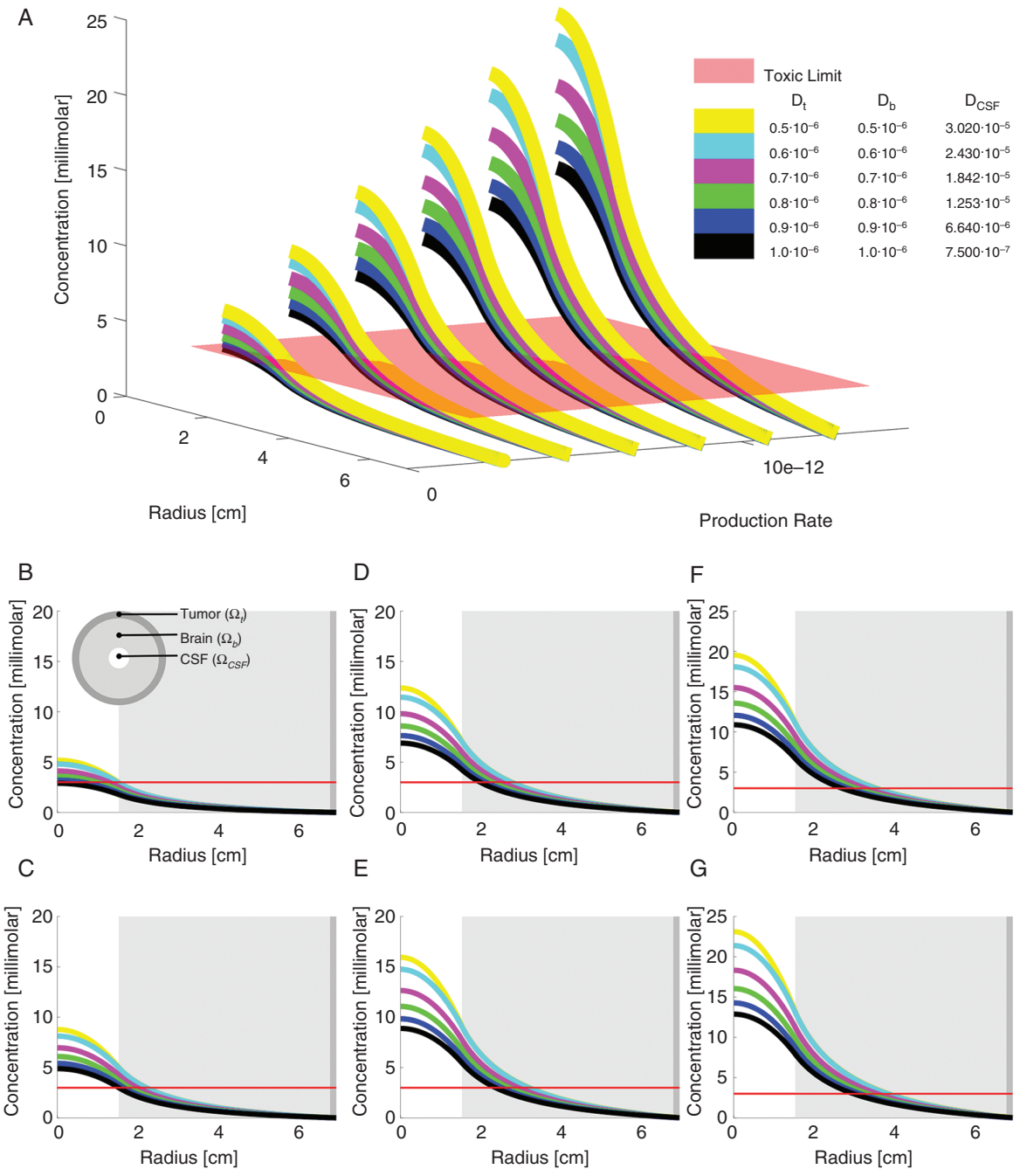

Fig. 3. Biometric study of differing D2HG release rates and diffusivities. Differential concentration profiles as a function of tissue diffusivity (D) and D2HG production rate (S_A) in the tumor. The diffusivities are color-coded as can be reviewed in panel A, where multiple concentration profiles are plotted against each other with differing D2HG diffusivities and production rates. Panels B–G show each D2HG S_A separately, as follows: (B) $S_A = 2.89 \times 10^{-12}$ mol/mL/sec; (C) $S_A = 4.89 \times 10^{-12}$; (D) $S_A = 6.88 \times 10^{-12}$; (E) $S_A = 8.88 \times 10^{-12}$; (F) $S_A = 10.87 \times 10^{-12}$; (G) $S_A = 12.87 \times 10^{-12}$. The red line is the toxic limit in the tissue, as indicated by the minimum D2HG concentration required to increase neuronal network bursts.[12] D_t = diffusion constant through tumor; D_b = diffusion constant through brain; D_{CSF} = diffusion constant through CSF.

of cancer, as articulated by Hanahan and Weinberg, including angiogenesis, invasion, metastasis, and immune modulation.[18] Aberrant cellular metabolism is also a critical step in malignant transformation, as demonstrated by the discovery that a large proportion of infiltrative gliomas, cartilaginous tumors, and acute myeloid leukemias (AMLs) contain function-altering point mutations in IDH1 or IDH2, leading to the production of D2HG instead of αKG.[2,19–23]

To date, the vast majority of studies on the effect of D2HG in IDH1^{mut} cancers have focused on its role within

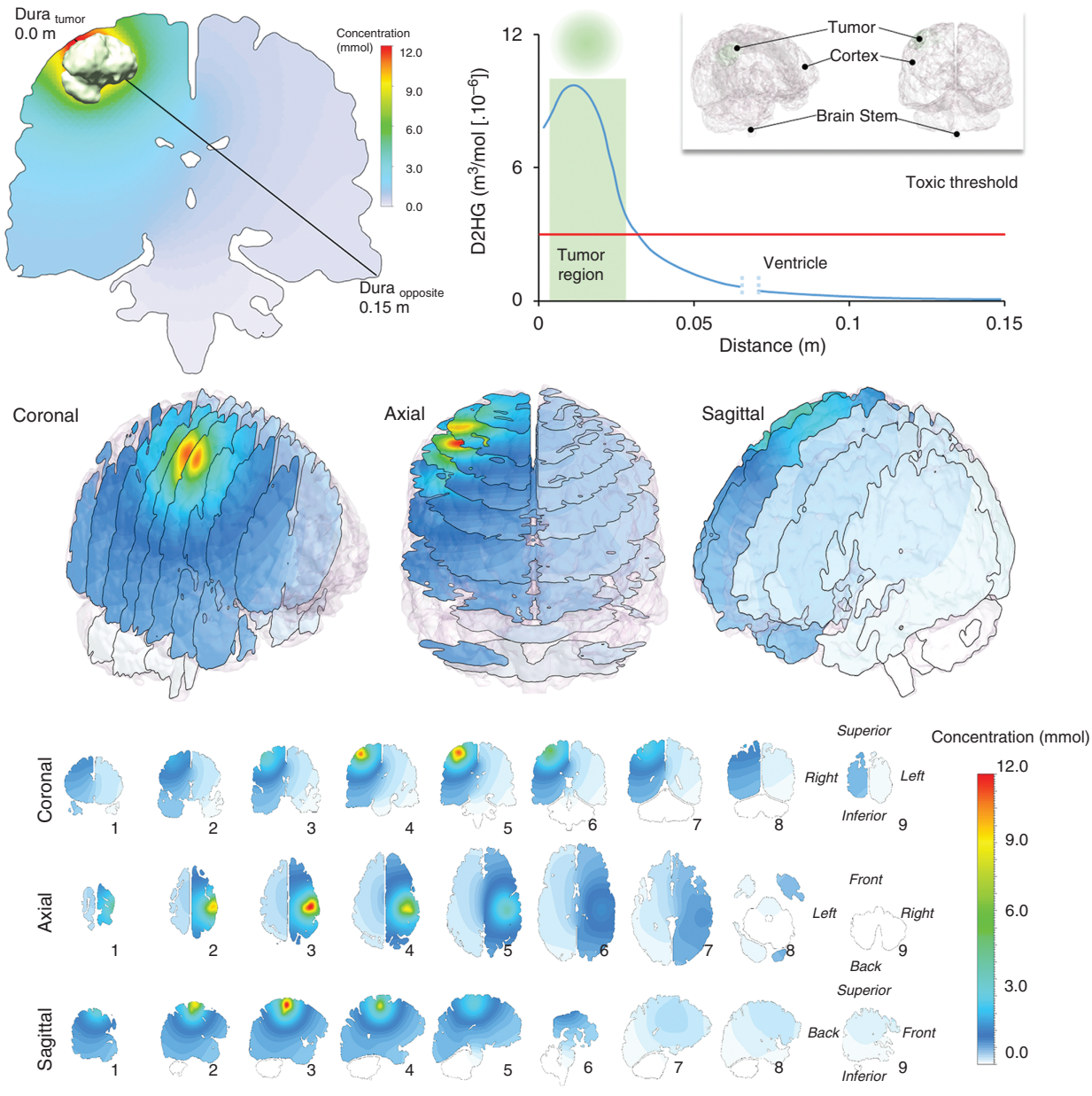

Fig. 4. Predicted D2HG concentration profiles around the IDH1mut glioma of patient 1. The concentration is drawn on cross-sectional planes overlaid inside the 3D structure. (Upper left) Axial cross-section cut located through the center of the tumor mass. Here, the black line corresponds to a raytrace through the tissue where a concentration profile can be observed and plotted (upper right) as a function of distance originating at the dura near the tumor surface (Dura $_{tumor}$) and terminating at the dura opposite the tumor surface (Dura $_{opposite}$). The gap in the concentration curve represents the CSF-filled ventricular space.

the tumor cell. D2HG competitively inhibits several DNA and histone demethylase enzymes that require αKG as a cofactor, leading to global DNA and histone hypermethylation,[1] which has been connected to suppression of cellular differentiation.[24] Indeed, IDH1mut generates a similar hypermethylation profile in chondrosarcomas, AML, glioma, and cholangiocarcinomas.[25] D2HG also increases the activity of EGLN1–3, leading to increased cellular immortalization, and can block hepatocyte nuclear factor 4α, which is required for the normal differentiation of hepatobiliary cells.[26–28] More recent studies found that D2HG blocks DNA repair enzymes, rendering IDH1mut cells more vulnerable to radiation and chemotherapy.[3,29]

While D2HG clearly has a wide range of effects within IDH1mut tumor cells, it can also be released by those tumor cells into the extracellular space. Artificial expression of R132H IDH1 in U87MG glioblastoma cells leads to a rapid accumulation of D2HG in the culture medium,[2] consistent with our data from cultured patient-derived glioma cells containing endogenous IDH1mut (Fig. 1). Elevated D2HG

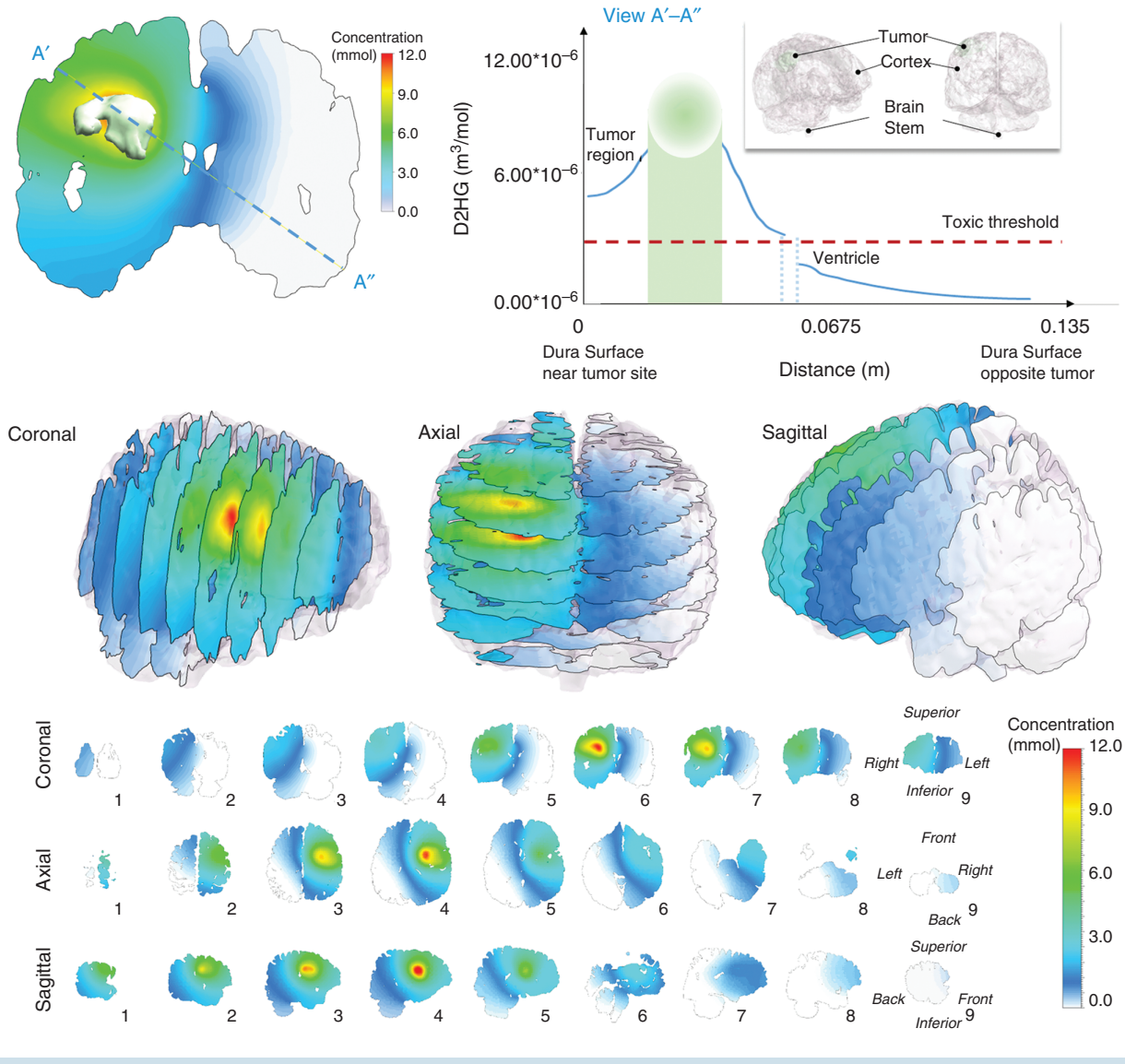

Fig. 5. Predicted D2HG concentration profiles around the IDH1^{mut} glioma of patient 2. The concentration is drawn on cross-sectional planes overlaid inside the 3D structure. (Upper left) Axial cross-section cut located through the center of the tumor mass. Here, the black line corresponds to a raytrace through the tissue where a concentration profile can be observed and plotted (upper right) as a function of distance originating at the dura near the tumor surface (Dura $_{tumor}$) and terminating at the dura opposite the tumor surface (Dura $_{opposite}$). The gap in the concentration curve represents the CSF-filled ventricular space.

has consistently been found in the peripheral serum of patients with systemic IDH1^{mut} malignancies.[30–36] Elevated D2HG is also readily detectable in the CSF of IDH1^{mut} glioma patients.[5] Together, these studies indicate that D2HG is released from IDH1^{mut} cells into surrounding tissues.

The next question, then, is whether and how D2HG affects the microenvironment of an IDH1^{mut} tumor—a subject that is drawing increased attention. Sasaki et al found that, in transgenic mice bearing nestin-driven IDH1^{mut}, D2HG disrupts the normal hydroxylation of collagen by αKG-dependent prolyl hydroxylases, causing disordered perivascular basement membranes.[37] Kohanbash et al reported that exogenous D2HG suppresses signal transducer and activator of transcription–dependent production of CXCL10, leading to reduced CD8+ cytotoxic T-cell recruitment to IDH1^{mut} gliomas and reduced vaccine efficacy.[6] A new RCAS/tva system of IDH1^{mut} gliomas by Amankulor et al showed broad suppression of immune cell recruitment, including fewer macrophages, monocytes, microglia, lymphocytes, neutrophils, and dendritic cells, compared with syngeneic IDH1^{wt} gliomas.[38] Previously, our group reported that IDH1^{mut} gliomas contain far fewer intratumoral microthrombi, and cause fewer distal venous thromboembolic complications, than their IDH1^{wt} counterparts.[13] One of the potential mechanisms is calcium-dependent suppression of platelet aggregation

Table 2. Model parameters used in the simulation of the reconstructed brain

Parameter	Symbol	Value	Units
CSF flow rate	q_{CSF}	5.79×10^{-9}	m^3/s
Production rate	S_A	4.89×10^{-12}	$mol/cm^3/s$
Diffusion coefficients in tumor	D_t	0.5×10^{-6}	cm^2/s
Diffusion coefficients in brain tissue	D_b	0.5×10^{-6}	cm^2/s
Diffusion coefficients in CSF space	D_{CSF}	30.2×10^{-6}	cm^2/s
Volume of brain tissue	V_b	1508	mL
Volume of tumor	V_t	7.2	mL
Volume of toxic region	V_{toxic}	110.8	mL

by D2HG. In fact, platelet function is so severely impaired in mice bearing IDH1^{mut} glioma xenografts, their bleeding time is increased at least tenfold over nontumor mice and mice bearing IDH1^{wt} xenografts.[13] We have also demonstrated that, whereas IDH1^{mut} gliomas are less likely to cause thrombosis, they are more likely to cause seizures in patients, and that D2HG increases synchronized network bursts in cultured cortical neurons through the ionotropic *N*-methyl-D-aspartate receptor.[12]

Thus far, most of the reported effects of D2HG in the IDH1^{mut} tumor microenvironment occur at low millimolar levels, raising the issue of whether D2HG reaches such concentrations in the extracellular space in and around an IDH1^{mut} tumor, especially a glioma. Prior studies on D2HG production showed that up to 30 mM D2HG was present within IDH1^{mut} tumor tissue homogenates and cell lysates, but such data are difficult to extrapolate to the extracellular compartment. Direct measurement of interstitial D2HG in vivo is also very difficult without some mechanical disruption of the cells, which would result in artefactual contamination by intracellular D2HG from damaged cells. Advanced radiographic methods can detect elevated D2HG within IDH1^{mut} tumors[39–42] but cannot distinguish intracellular from extracellular D2HG. To address this in a noninvasive manner, we calculated the in vitro D2HG release rate from 2 patient-derived gliomas with the most common IDH1 mutation, R132H, and extrapolated the results to an estimated average volume of an IDH1^{mut} glioma in a patient. This suggested that there may be a relatively broad range of D2HG release in an IDH1^{mut} glioma, from approximately 3.2–83.0 $\times 10^{-12}$ moles of D2HG per second.

Independent of these in vitro–based studies, we used mathematical models of fluid flow throughout the intracerebral compartment to calculate the amount of D2HG that an IDH1^{mut} glioma would have to release in order to generate the range of CSF concentrations reported by Kalinina et al.[5] This modeling accounted for as many variables as possible, including expected rates of D2HG diffusion and CSF turnover. Models yielding intratumoral D2HG concentrations that exceeded the known range of D2HG within tumor tissue homogenates were discarded. The result was an estimated rate of D2HG release of 2.9–12.9 $\times 10^{-12}$ mol/sec, which matched the lower end of the estimated range based on cultured cells. These complementary approaches have, for the first time, produced evidence-based estimates of D2HG release by an IDH1^{mut} glioma into its microenvironment. Our models suggest that as much as 3 mM D2HG may be present in the interstitial fluid of an IDH1^{mut} glioma, up to 2 cm away from the tumor center.

While these approaches to estimating D2HG release are useful, some postulates were required that produced inevitable caveats. Prior patient-based work showed that overall D2HG production in IDH1^{mut} gliomas increases with tumor grade, cell proliferation, and tumor density.[43] The IDH1^{mut} cells used in our study were from grades III–IV gliomas, as grade II IDH1^{mut} gliomas are notoriously difficult to culture in vitro, and our efforts to do so have been unsuccessful thus far. Therefore, the cell-based data may not fully represent the D2HG release rates seen in grade II gliomas, which may be lower than grades III–IV gliomas. However, these IDH1^{mut} glioma cell lines still grow slower than the IDH1^{wt} cells (average 1.5-fold increase in IDH1^{mut} cells over 1 wk vs 3.1-fold in IDH1^{wt} cells) as well as the IDH1^{mut} HT1080 fibrosarcoma cells (4.3-fold). There also did not appear to be a consistent positive correlation between cell proliferation and D2HG release among IDH1^{mut} cells, since TB09 showed a 2.7-fold increase in cell number over 1 week, whereas GBM196 showed essentially no proliferation over that same time period, yet the latter cells released much more D2HG in the same culture conditions (Fig. 1). This is interesting in its own right, as it suggests that other cell-based variables must be greatly affecting D2HG production and efflux, apart from proliferation. Nevertheless, the lack of in vitro data from grade II IDH1^{mut} gliomas means that the current study may not accurately represent D2HG in the microenvironment of grade II gliomas. In patients, diffusely infiltrative gliomas show decreasing cell density with increasing distance from the tumor center. Furthermore, cell density at the tumor center, as well as the extent of change in cell density as a function of distance from the tumor center, varies according to differences in glioma grade, tumor cell invasiveness, and tumor location. But because it is very difficult to accurately account for these variables, an

artificially discrete tumor:nontumor interface was used in the mathematical modeling. We also assumed that none of the D2HG released by tumor cells is bound to or taken up by admixed nonneoplastic cells, such as neurons and astrocytes. Finally, it was assumed that extracellular D2HG is stable and is not rapidly degraded outside the cell in a human brain. Further investigations into the interaction of D2HG with nonneoplastic elements in a glioma are ongoing, and may help further refine this model.

To our knowledge, this study is the first to quantify and model D2HG release by IDH1^{mut} gliomas. Our results suggest that relatively large concentrations of D2HG, in the low millimolar range, may be present in and around an IDH1^{mut} glioma. Because a number of estimates and assumptions had to be coupled to the experimental data, this postulated concentration gradient is relatively broad, and in particular may not hold for grade II gliomas, which tend to have lower cell density and are less proliferative and infiltrative. Still, this provides a foundation on which to base future evaluation of D2HG in the tumor microenvironment, including mechanisms of D2HG efflux from tumor cells, its effects on nonneoplastic cells, and a greater understanding of the therapeutic consequences of drugs that block IDH1^{mut} enzyme activity and decrease D2HG production.

Supplementary material

Supplementary material is available at *Neuro-Oncology* online.

Funding

A.L., K.T., and G.A.H. were supported by NSF CBET1403409. C.D.J. was supported by NIH R01NS095642. J.N.S. was supported by NIH R01CA176830, R01CA184320, and R24NS092940. C.H. was supported by NIH K08CA155764 and R01NS102669.

Acknowledgments

The authors thank Dr Hai Yan for providing TB09 cells. LC-MS analyses were done at the University of Illinois at Chicago Mass Spectrometry, Metabolomics & Proteomics Facility.

Conflict of interest statement. The authors declare no potential conflicts of interest.

References

1. Horbinski C. What do we know about IDH1/2 mutations so far, and how do we use it? *Acta Neuropathol*. 2013;125(5):621–636.
2. Dang L, White DW, Gross S, et al. Cancer-associated IDH1 mutations produce 2-hydroxyglutarate. *Nature*. 2009;462(7274):739–744.
3. Sulkowski PL, Corso CD, Robinson ND, et al. 2-Hydroxyglutarate produced by neomorphic IDH mutations suppresses homologous recombination and induces PARP inhibitor sensitivity. *Sci Transl Med*. 2017;9(375):doi: 10.1126/scitranslmed.aal2463.
4. Luchman HA, Stechishin OD, Dang NH, et al. An in vivo patient-derived model of endogenous IDH1-mutant glioma. *Neuro Oncol*. 2012;14(2):184–191.
5. Kalinina J, Ahn J, Devi NS, et al. Selective detection of the D-enantiomer of 2-hydroxyglutarate in the CSF of glioma patients with mutated isocitrate dehydrogenase. *Clin Cancer Res*. 2016;22(24):6256–6265.
6. Kohanbash G, Carrera DA, Shrivastav S, et al. Isocitrate dehydrogenase mutations suppress STAT1 and CD8+ T cell accumulation in gliomas. *J Clin Invest*. 2017;127(4):1425–1437.
7. Gilbert MR, Liu Y, Neltner J, et al. Autophagy and oxidative stress in gliomas with IDH1 mutations. *Acta Neuropathol*. 2014;127(2):221–233.
8. Liu Y, Gilbert MR, Kyprianou N, Rangnekar VM, Horbinski C. The tumor suppressor prostate apoptosis response-4 (Par-4) is regulated by mutant IDH1 and kills glioma stem cells. *Acta Neuropathol*. 2014;128(5):723–732.
9. Reitman ZJ, Jin G, Karoly ED, et al. Profiling the effects of isocitrate dehydrogenase 1 and 2 mutations on the cellular metabolome. *Proc Natl Acad Sci U S A*. 2011;108(8):3270–3275.
10. Latini A, da Silva CG, Ferreira GC, et al. Mitochondrial energy metabolism is markedly impaired by D-2-hydroxyglutaric acid in rat tissues. *Mol Genet Metab*. 2005;86(1-2):188–199.
11. Latini A, Scussiato K, Rosa RB, et al. D-2-hydroxyglutaric acid induces oxidative stress in cerebral cortex of young rats. *Eur J Neurosci*. 2003;17(10):2017–2022.
12. Chen H, Judkins J, Thomas C, et al. Mutant IDH1 and seizures in patients with glioma. *Neurology*. 2017;88(19):1805–1813.
13. Unruh D, Schwarze SR, Khoury L, et al. Mutant IDH1 and thrombosis in gliomas. *Acta Neuropathol*. 2016;132(6):917–930.
14. Ward PS, Lu C, Cross JR, et al. The potential for isocitrate dehydrogenase mutations to produce 2-hydroxyglutarate depends on allele specificity and subcellular compartmentalization. *J Biol Chem*. 2013;288(6):3804–3815.
15. Mazor T, Chesnelong C, Pankov A, et al. Clonal expansion and epigenetic reprogramming following deletion or amplification of mutant IDH1. *Proc Natl Acad Sci U S A*. 2017;114(40):10743–10748.
16. Del Monte U. Does the cell number 10(9) still really fit one gram of tumor tissue? *Cell Cycle*. 2009;8(3):505–506.
17. Chen H, Judkins J, Thomas C, et al. Mutant IDH1 and seizures in patients with glioma. *Neurology*. 2017;88(19):1805–1813.
18. Hanahan D, Weinberg RA. Hallmarks of cancer: the next generation. *Cell*. 2011;144(5):646–674.
19. Parsons DW, Jones S, Zhang X, et al. An integrated genomic analysis of human glioblastoma multiforme. *Science*. 2008;321(5897):1807–1812.
20. Yan H, Parsons DW, Jin G, et al. IDH1 and IDH2 mutations in gliomas. *N Engl J Med*. 2009;360(8):765–773.
21. Amary MF, Bacsi K, Maggiani F, et al. IDH1 and IDH2 mutations are frequent events in central chondrosarcoma and central and periosteal chondromas but not in other mesenchymal tumours. *J Pathol*. 2011;224(3):334–343.
22. Borger DR, Tanabe KK, Fan KC, et al. Frequent mutation of isocitrate dehydrogenase (IDH)1 and IDH2 in cholangiocarcinoma identified through broad-based tumor genotyping. *Oncologist*. 2012;17(1):72–79.
23. Mardis ER, Ding L, Dooling DJ, et al. Recurring mutations found by sequencing an acute myeloid leukemia genome. *N Engl J Med*. 2009;361(11):1058–1066.

24. Lu C, Ward PS, Kapoor GS, et al. IDH mutation impairs histone demethylation and results in a block to cell differentiation. *Nature*. 2012;483(7390):474–478.
25. Guilhamon P, Eskandarpour M, Halai D, et al. Meta-analysis of IDH-mutant cancers identifies EBF1 as an interaction partner for TET2. *Nat Commun*. 2013;4:2166.
26. Koivunen P, Lee S, Duncan CG, et al. Transformation by the (R)-enantiomer of 2-hydroxyglutarate linked to EGLN activation. *Nature*. 2012;483(7390):484–488.
27. Losman JA, Looper RE, Koivunen P, et al. (R)-2-hydroxyglutarate is sufficient to promote leukemogenesis and its effects are reversible. *Science*. 2013;339(6127):1621–1625.
28. Saha SK, Parachoniak CA, Ghanta KS, et al. Mutant IDH inhibits HNF-4α to block hepatocyte differentiation and promote biliary cancer. *Nature*. 2014;513(7516):110–114.
29. Lu Y, Kwintkiewicz J, Liu Y, et al. Chemosensitivity of IDH1-mutated gliomas due to an impairment in PARP1-mediated DNA repair. *Cancer Res*. 2017;77(7):1709–1718.
30. Balss J, Pusch S, Beck AC, et al. Enzymatic assay for quantitative analysis of (D)-2-hydroxyglutarate. *Acta Neuropathol*. 2012;124(6):883–891.
31. Sellner L, Capper D, Meyer J, et al. Increased levels of 2-hydroxyglutarate in AML patients with IDH1-R132H and IDH2-R140Q mutations. *Eur J Haematol*. 2010;85(5):457–459.
32. Fathi AT, Sadrzadeh H, Borger DR, et al. Prospective serial evaluation of 2-hydroxyglutarate, during treatment of newly diagnosed acute myeloid leukemia, to assess disease activity and therapeutic response. *Blood*. 2012;120(23):4649–4652.
33. Fathi AT, Sadrzadeh H, Comander AH, et al. Isocitrate dehydrogenase 1 (IDH1) mutation in breast adenocarcinoma is associated with elevated levels of serum and urine 2-hydroxyglutarate. *Oncologist*. 2014;19(6):602–607.
34. Borger DR, Goyal L, Yau T, et al. Circulating oncometabolite 2-hydroxyglutarate is a potential surrogate biomarker in patients with isocitrate dehydrogenase-mutant intrahepatic cholangiocarcinoma. *Clin Cancer Res*. 2014;20(7):1884–1890.
35. Janin M, Mylonas E, Saada V, et al. Serum 2-hydroxyglutarate production in IDH1- and IDH2-mutated de novo acute myeloid leukemia: a study by the Acute Leukemia French Association group. *J Clin Oncol*. 2014;32(4):297–305.
36. DiNardo CD, Propert KJ, Loren AW, et al. Serum 2-hydroxyglutarate levels predict isocitrate dehydrogenase mutations and clinical outcome in acute myeloid leukemia. *Blood*. 2013;121(24):4917–4924.
37. Sasaki M, Knobbe CB, Itsumi M, et al. D-2-hydroxyglutarate produced by mutant IDH1 perturbs collagen maturation and basement membrane function. *Genes Dev*. 2012;26(18):2038–2049.
38. Amankulor NM, Kim Y, Arora S, et al. Mutant IDH1 regulates the tumor-associated immune system in gliomas. *Genes Dev*. 2017;31(8):774–786.
39. de la Fuente MI, Young RJ, Rubel J, et al. Integration of 2-hydroxyglutarate-proton magnetic resonance spectroscopy into clinical practice for disease monitoring in isocitrate dehydrogenase-mutant glioma. *Neuro Oncol*. 2016;18(2):283–290.
40. Andronesi OC, Loebel F, Bogner W, et al. Treatment response assessment in IDH-mutant glioma patients by noninvasive 3D functional spectroscopic mapping of 2-hydroxyglutarate. *Clin Cancer Res*. 2016;22(7):1632–1641.
41. Chaumeil MM, Larson PE, Yoshihara HA, et al. Non-invasive in vivo assessment of IDH1 mutational status in glioma. *Nat Commun*. 2013;4:2429.
42. Elkhaled A, Jalbert LE, Phillips JJ, et al. Magnetic resonance of 2-hydroxyglutarate in IDH1-mutated low-grade gliomas. *Sci Transl Med*. 2012;4(116):116ra115.
43. Choi C, Raisanen JM, Ganji SK, et al. Prospective longitudinal analysis of 2-hydroxyglutarate magnetic resonance spectroscopy identifies broad clinical utility for the management of patients with IDH-mutant glioma. *J Clin Oncol*. 2016;34(33):4030–4039.